Inorganica Chimica Acta, *194* (1992) 163–170

Preparation and structural characterization of three tetrakis(triazeno)diruthenium compounds

F. Albert Cotton*, Larry R. Falvello, Tong Ren and K. Vidyasagar

Department of Chemistry and Laboratory for Molecular Structure and Bonding, Texas A&M University, College Station, TX 77843 (USA)

(Received November 20, 1991)

Abstract

Three closely related diruthenium triazeno complexes, $Ru_2[(p\text{-tolyl})NNN(p\text{-tolyl})]_4(CH_3CN)$ (**1**), $Ru_2(PhNNNPh)_4$ (**2**) and $Ru_2[(p\text{-tolyl})NNN(p\text{-tolyl})]_4(CH_3CN)\cdot BF_4$ (**3**), have been synthesized and structurally characterized. Direct cocrystallization of $Ru_2[(p\text{-tolyl})NNN(p\text{-tolyl})]_4$ with CH_3CN affords the dark red **1** in space group $P4/n$ with $a=14.851(3)$, $c=11.942(7)$ Å, $V=2634(2)$ Å^3 and $Z=2$. The purple **2** was crystallized in space group $P\bar{1}$ *with* $a=13.720(5)$, $b=15.901(4)$, $c=10.388(4)$ Å, $\alpha=103.92(3)$, $\beta=94.56(3)$, $\gamma=99.11(3)°$, $V=2155(1)$ Å^3 and $Z=2$. The dark green **3** was obtained by oxidizing $Ru_2[(p\text{-tolyl})NNN(p\text{-tolyl})]_4$ with $Ag(CH_3CN)_4BF_4$, and crystallized in space group $P2/n$ with $a=13.280(2)$, $b=16.816(5)$, $c=13.095(4)$ Å, $\beta=90.16(2)°$, $V=2924(2)$ Å^3 and $Z=2$. The Ru–Ru bond lengths determined through diffraction studies are 2.407(1), 2.3994(6) and 2.373(1) Å for **1**, **2** and **3**, respectively. The results of both magnetic susceptibility and EPR measurements on **3** consistently confirm a π^{*3} ground state configuration as previously predicted.

Introduction

This report makes a further contribution to our understanding of the electronic structures and other properties of diruthenium species of the types $Ru_2(LL)_4$ and $Ru_2(LL)_4X$, where LL is a bridging bidentate, anionic ligand such as carboxylate, hydroxypyridinate (xhp^-), amidinate ($RNCR'NR^-$) or triazenate ($RNNNR^-$).

While the ground-state electronic structures of dinuclear compounds of this type with 6, 7, 8 or 9 electrons involved in the metal–metal interaction have never been ambiguous because the level order $\sigma<\pi<\delta<\delta^*$ is always followed, the diruthenium species, which have either 11 or 12 electrons have, from the start, posed problems [1]. Once eight electrons have been assigned to provide a $\sigma^2\pi^4\delta^2$ configuration, the problem of how to assign the remaining three or four electrons remains. It is not straightforward because three possibilities have to be considered for the ordering of the δ^* and π^* orbitals: $\delta^*<\pi^*$, or $\delta^*\approx\pi^*$, or $\pi^*<\delta^*$. Previous work on this problem has shown that the ordering of these levels is markedly influenced by the LL ligands present. The less basic ligands, RCO_2^- and xhp^-, favor the $\delta^*\approx\pi^*$ situation, with the result that Ru_2^{5+} systems have quartet ground states based on a $\pi^{*2}\delta^*$ configuration and the Ru_2^{4+} compounds have $\delta^{*2}\pi^{*2}$ configurations, as shown by the structural and magnetic data [2, 3]. With the more basic ligands, the relatively limited data available so far (three compounds structurally characterized) [4–6], with support from theory [6, 7], has led to the conclusion that the level ordering is $\pi^*<\delta^*$ so that Ru_2^{5+} and Ru_2^{4+} compounds should have π^{*3} and π^{*4} configurations, respectively. In this report, we double the data base by providing three more structurally characterized compounds.

Experimental

Standard vacuum-line and Schlenk techniques were used exclusively to carry out the various syntheses under an argon atmosphere. All solvents used were of reagent grade or better from commercial sources and freshly distilled under N_2 from suitable drying reagents. The compounds $Ru_2(PhN_3Ph)_4$ (**2**) and $Ru_2(p\text{-tolN}_3p\text{-tol})_4$ (**4**) were prepared according to the literature [4, 8].

Syntheses

$Ru_2(p\text{-tolN}_3p\text{-tol})_4(CH_3CN)$ (1)

To a benzene solution of 0.22 g $Ru_2(p\text{-tolN}_3p\text{-tol})_4$ (*c.* 10 ml) was added 0.5 ml CH_3CN, and then 15 ml hexane was slowly layered on the top. Long column-

---

*Author to whom correspondence should be addressed.

0020-1693/92/$5.00

like crystals (1) appeared in two weeks, and one of them was selected for the X-ray diffraction study.

$Ru_2(PhN_3Ph)_4$ (2)

The complex was recrystallized twice from hot toluene to give a purple microcrystalline material. A saturated benzene solution of this purified compound was then layered with hexane. A large quantity of crystals (2) of X-ray quality was harvested after two weeks.

$[Ru_2(p\text{-}tolN_3p\text{-}tol)_4(CH_3CN)]BF_4$ (3)

A Schlenk tube was charged with 0.11 g $Ru_2(p\text{-}tolN_3p\text{-}tol)_4$ (0.10 mmol) and 0.040 g $Ag(CH_3CN)_4 \cdot BF_4$ (0.11 mmol), to which 10 ml CH_2Cl_2 was added with vigorous stirring. The purple color of the (II,II) compound **2** turned to green immediately upon the addition of CH_2Cl_2. The solution was stirred for 1 h before it was filtered through a celite column to remove the Ag precipitate. The filtrate was concentrated to 5 ml under vacuum, and then layered with 15 ml of Et_2O. A large quantity of the plate-like crystals (3) formed in a week. They were filtered and air-dried. The yield was almost quantitative (always above 95%).

UV–Vis (CH_2Cl_2): 756 nm (15 300 M^{-1} cm^{-1}), 332 nm (53 300 M^{-1} cm^{-1}). IR (cm^{-1}): 1601(m), 1283(s), 1213(s), 1180(m), 1114(w), 1090(m), 1051(s), 877(w), 818(s), 722(w), 591(m), 525(m), 478(m). The measured susceptibility is $\chi_g = 6.62 \times 10^{-7}$ cgs at 298 K. The corresponding effective magnetic moment (μ_{eff}) after the diamagnetic correction ($\chi_D = 670 \times 10^{-6}$ cgs mol^{-1} for the complex) is 1.88 μ_B.

Physical measurements

The UV–Vis spectra were measured on a Cary 17D spectrometer at ambient temperature. The IR spectra were recorded on an IBM IR/44 FT-IR instrument having a range 4000–400 cm^{-1}. The spectra of the solid samples were taken as Nujol mulls between CsI plates. Room temperature magnetic susceptibility was determined on a Johnson Matthey MSB 1 magnetic susceptibility balance (calibrated with $HgCo(SCN)_4$). The ESR spectrum of a frozen CH_2Cl_2 solution of **3** was recorded at 77 K on an IBM Instruments, Inc., ER200D-SRC spectrometer.

X-ray crystallography

The description of the equipment and the detailed discussion of the normal crystallographic procedures we followed are presented elsewhere [9, 10]. No decay was observed for any of the data sets. Hence they were corrected only for Lorentz and polarization effects as well as absorption effects. The absorption corrections were done by the empirical ψ-scan method [11].

$Ru_2(p\text{-}tolN_3p\text{-}tol)_4(CH_3CN)$ (1)

A dark red columnar crystal was attached to the top of a quartz fiber with epoxy cement. The crystal was kept at −60 °C during the data collection. Indexing revealed a tetragonal cell. The Laue symmetry was shown to be *4/m* rather than *4/mmm* by normal-beam oscillation photographs. The systematic absences of the diffraction data indicated that the space group was *P4/n* (No. 85). The X-ray data were gathered on an Enraf-Nonius CAD4 diffractometer using monochromated Mo Kα radiation.

The positions of the Ru atoms were determined by the Patterson map obtained from SHELXS-86 [12a]. An alternating series of difference Fourier maps and full matrix least-squares refinements in the SDP [13] revealed the locations of all the other non-hydrogen atoms. All the non-hydrogen atoms were refined with anisotropic thermal parameters to convergence. The ruthenium atoms as well as the axial acetonitrile molecule reside on the crystallographic four-fold axis, and only one of the bridging ligands was required to complete the asymmetric unit. Although most of the hydrogen atoms could be seen in the final Fourier map, they were not included in any of the least-squares refinements. However, none of the hydrogen atoms on the methyl group of acetonitrile was found. They are probably disordered by the four-fold symmetry.

$Ru_2(PhN_3Ph)_4$ (2)

A dark purple parallelepiped was mounted on the top of a glass fiber with epoxy cement. A triclinic cell was determined based on the indexing of 23 reflections with $24.5 \leqslant 2\theta \leqslant 28°$. The data collection was carried out at room temperature on a Syntex P$\bar{1}$ diffractometer equipped with monochromated Mo Kα radiation. The structure was solved and refined in the same fashion as that for **1** in SDP. No interstitial solvent was found. All atoms were refined with anisotropic thermal parameters.

$[Ru_2(p\text{-}tolN_3p\text{-}tol)_4(CH_3CN)]BF_4$ (3)

A dark green plate was mounted on the top of a glass fiber with epoxy cement. The unit cell was determined to be monoclinic based on the indexing of 25 reflections with $26 \leqslant 2\theta \leqslant 35°$ and the axial photographs. The space group could be either *Pn* or *P2/n* according to the systematic absences, but the latter was proved to be the correct one by the successful refinement of the structure. The diffraction data were collected on an AFC5R Rigaku diffractometer equipped with monochromated Mo Kα radiation.

The ruthenium atoms were located by the use of a three-dimensional Patterson function. Both of them were located on a crystallographic two-fold axis. The remaining non-hydrogen atoms on the bridging ligands

TABLE 1. Crystal data for the three compounds

	$Ru_2[(tol)NNN(tol)]_4 \cdot CH_3CN$	$Ru_2(PhN_3Ph)_4$	$[Ru_2(tolNNNtol)_4(CH_3CN)]BF_4$
Formula	$Ru_2N_{13}C_{58}H_{59}$	$Ru_2N_{12}C_{48}H_{40}$	$Ru_2F_4N_{13}C_{58}BH_{59}$
Formula weight	1140.3	987.1	1227.2
Space group	$P4/n$	$P\bar{1}$ (No. 2)	$P2/n$ (No. 13)
a (Å)	14.851(3)	13.720(5)	13.280(2)
b (Å)		15.901(4)	16.816(5)
c (Å)	11.942(7)	10.388(4)	13.095(4)
α (°)		103.92(3)	
β (°)		94.56(3)	90.16(2)
γ (°)		99.11(3)	
V (Å^3)	2634(2)	2155(1)	2924(2)
Z	2	2	2
D_{calc} (g/cm^3)	1.438	1.521	1.394
Crystal size (mm)	0.25×0.20×0.15	0.70×0.35×0.25	0.30×0.30×0.15
μ(Mo Kα) (cm^{-1})	6.2	7.3	5.7
Data collection instrument	Enraf-Nonius CAD-4	Syntex P$\bar{1}$	Rigaku AFC5R
Radiation monochromated in incident beam (Mo Kα, Å)	0.71073	0.71073	0.71073
Orientation reflections: no.; range (2θ)	25; $30<2\theta\leq40$	23; $24.5<2\theta\leq28$	25; $26<2\theta\leq35$
Temperature (°C)	−60	20	20
Scan method	2θ–ω	2θ–ω	2θ–ω
Data collection range, 2θ (°)	$4\leq2\theta\leq50$	$4\leq2\theta\leq46$	$2\leq2\theta\leq50$
No. unique data, total with $F^2_o>3\sigma(F^2_o)$	2320, 1682	5516, 4906	5191, 2390
No. of parameters refined	202	559 (see text)	419
Transmission factors: max., min.	0.98, 0.88	1.00, 0.96	1.00, 0.74
R[a]	0.031	0.040	0.058
R_w[b]	0.042	0.061	0.066
Quality-of-fit indicator[c]	1.313	1.907	1.148
Largest shift/e.s.d., final cycle	0.32	0.02	0.18
Largest peak (e/Å^3)	0.45	0.61	1.67

[a] $R=\Sigma||F_o|-|F_c||/\Sigma|F_o|$. [b] $R_w=[\Sigma w(|F_o|-|F_c|)^2/\Sigma w|F_o|^2]^{1/2}$; $w=1/\sigma^2(|F_o|)$. [c] Quality-of-fit $=[\Sigma w(|F_o|-|F_c|)^2/(N_{observed}-N_{parameters})]^{1/2}$.

were introduced and refined by an alternating series of difference Fourier maps and least-squares refinements. An acetonitrile molecule was then found at one of the axial positions of the metal core. Later the peaks corresponding to the BF_4 anion were also located with the B atom and one F atom lying on the two-fold axis and the other three F atoms disordered over two sets of positions related by the two-fold symmetry. Further constrained refinement with the disordered anion was carried out in SHELX-76 [12b]. In the final least-squares refinement, hydrogen atoms were included at the calculated positions with fixed displacement parameters, but were not refined.

Crystallographic and procedural data for all aforementioned structures are presented in Table 1, and the positional parameters are listed in Tables 2, 3 and 4 for **1**, **2** and **3**, respectively.

Results and discussion

In contrast to the earlier observation for the analogous complex $Ru_2(PhN_3Ph)_4$ [8] the axial acetonitrile adduct of $Ru_2(p\text{-tolN}_3p\text{-tol})_4$ is readily formed during the crystallization. The crystallization of $Ru_2(PhN_3Ph)_4$ is also easily achieved by working with a purified sample.

A reversible oxidation was observed at 0.28 V for $Ru_2(p\text{-tolN}_3p\text{-tol})_4$ from an earlier CV study [4], and thus the oxidation of this compound with Ag^+ salt was expected to be feasible. As revealed by the result of the X-ray diffraction study, the product from our oxidation reaction contained an axial ligand CH_3CN, which was introduced by the use of $Ag(CH_3CN)_4BF_4$. Attempts to crystallize the cation free of any axial ligand with BF_4^-, PF_6^- counter ions or even larger ones such as BPh_4^- and $B_{11}CH_{12}^-$ were unsuccessful.

The geometry of the neutral $Ru_2(p\text{-tolN}_3p\text{-tol})_4(CH_3CN)$ (**1**) is given in Fig. 1. From this ORTEP drawing and the selected bond distances and angles (Table 5) it can be seen that the basic features of **1** are almost the same as those of the one without axial ligation (**4**) [4]. The average Ru–N (2.055(3) Å) is within 3σ range of that for **4** (2.04(1) Å). The Ru–Nσ bonds are thus not influenced by the axial ligation (or we could say there is no first-order structural perturbation). However, the torsional angle N(1)–

TABLE 2. Positional parameters and their e.s.d.s for $Ru_2[(tol)NNN(tol)]_4 \cdot CH_3CN$

Atom	x	y	z	B (Å^2)
Ru(1)	0.250	0.250	0.15200(4)	1.552(6)
Ru(2)	0.250	0.250	0.35359(4)	1.583(6)
N(1)	0.2541(2)	0.1115(2)	0.1655(2)	1.77(5)
N(2)	0.2838(2)	0.0698(2)	0.2542(2)	1.95(5)
N(3)	0.2940(2)	0.1198(2)	0.3440(2)	1.81(5)
N(4)	0.250	0.250	−0.0249(5)	2.51(8)
C(1)	0.2442(2)	0.0498(2)	0.0737(3)	1.90(6)
C(2)	0.3048(2)	−0.0192(2)	0.0536(3)	2.55(7)
C(3)	0.2954(3)	−0.0744(2)	−0.0386(3)	2.92(7)
C(4)	0.1725(2)	0.0611(2)	0.0003(3)	2.50(6)
C(5)	0.1638(2)	0.0054(2)	−0.0916(3)	2.76(7)
C(6)	0.2257(3)	−0.0622(2)	−0.1140(3)	2.70(7)
C(7)	0.2164(3)	−0.1207(3)	−0.2165(3)	3.95(9)
C(8)	0.3305(2)	0.0688(2)	0.4349(3)	2.00(6)
C(9)	0.3662(3)	0.1149(2)	0.5244(3)	3.15(8)
C(10)	0.4060(3)	0.0691(3)	0.6130(3)	3.65(8)
C(11)	0.3324(3)	−0.0245(2)	0.4362(3)	3.05(7)
C(12)	0.3730(3)	−0.0690(2)	0.5257(3)	3.48(8)
C(13)	0.4105(3)	−0.0236(3)	0.6146(3)	2.97(7)
C(14)	0.4568(3)	−0.0724(3)	0.7101(3)	3.86(8)
C(15)	0.250	0.250	−0.1212(6)	3.3(1)
C(16)	0.250	0.250	−0.2452(8)	9.6(2)

Anisotropically refined atoms are given in the form of the equivalent isotropic displacement parameter defined as: (4/3)-$[a^2\beta_{11}+b^2\beta_{22}+c^2\beta_{33}+ab(\cos\gamma)\beta_{12}-ac(\cos\beta)\beta_{13}+bc(\cos\alpha)\beta_{23}]$.

Ru(1)–Ru(2)–N(3) has increased from almost zero (the average for **4** is 0.5(5)°) in **4** to 17.0(1)° in **1**, which reflects a significant second-order structural perturbation induced by the packing of the tolyl groups in the presence of the axial CH_3CN. The other related molecular dimensions are collected in Table 5.

The most interesting molecular dimension, the Ru–Ru distance of 2.407(1) Å, is 0.01 Å shorter than that in **4**. Usually axial ligation will cause a lengthening of the M–M bond, since σ donation from an axial ligand usually introduces a considerable amount of electron density into the σ^* orbital of the metal core. Another notable feature is that the Ru(2)–N(4) distance (2.113(6) Å) is 0.08 Å shorter than that in $Rh_2(CH_3CN)_{10}^{4+}$ (2.191 Å) [14] and much shorter than that in $Mo_2(CH_3CN)_{10}^{4+}$ (2.600 Å) [15]. Acetonitrile is known to be a moderate σ donor and a poor to moderate π acceptor. The shortness of both Ru–Ru and Ru–N_{ax} suggests that there is a moderate π backdonation from the π^* orbital of the metal core to the empty π^* orbital of acetonitrile besides the moderate σ donation, and this may cancel the potential lengthening of the M–M distance due to the σ donation. Such backdonation is plausible, since it is well known that the monomeric low spin Ru(II) amine complexes are all good π donors [16]. However, it is not clear why the bis-acetonitrile adduct was not formed.

TABLE 3. Positional parameters and their e.s.d.s for $Ru_2(PhN_3Ph)_4$

Atom	x	y	z	B (Å^2)
Ru(1)	0.20541(3)	0.32295(3)	0.23692(4)	2.333(9)
Ru(2)	0.27430(3)	0.19803(3)	0.13107(4)	2.380(9)
N(1)	0.3229(3)	0.3552(3)	0.3819(4)	2.63(9)
N(2)	0.4032(3)	0.3203(3)	0.3700(4)	2.81(9)
N(3)	0.3999(3)	0.2571(3)	0.2610(4)	2.83(9)
N(4)	0.1361(3)	0.2443(3)	0.3430(4)	2.44(9)
N(5)	0.1569(3)	0.1673(3)	0.3484(4)	2.81(9)
N(6)	0.2194(3)	0.1375(3)	0.2668(4)	2.57(9)
N(7)	0.0924(3)	0.2805(3)	0.0851(4)	2.55(9)
N(8)	0.0781(3)	0.2041(3)	−0.0030(4)	3.1(1)
N(9)	0.1448(3)	0.1547(3)	0.0083(4)	2.69(9)
N(10)	0.2900(3)	0.3904(3)	0.1255(4)	2.70(9)
N(11)	0.3245(3)	0.3506(3)	0.0178(4)	2.9(1)
N(12)	0.3173(3)	0.2653(3)	−0.0026(4)	2.82(9)
C(1)	0.3316(4)	0.4219(3)	0.5050(5)	2.9(1)
C(2)	0.4195(4)	0.4550(4)	0.5906(5)	3.6(1)
C(3)	0.4205(5)	0.5233(4)	0.7051(6)	4.2(1)
C(4)	0.3365(5)	0.5572(4)	0.7355(6)	4.3(2)
C(5)	0.2477(5)	0.5225(4)	0.6494(6)	4.0(1)
C(6)	0.2443(4)	0.4552(4)	0.5348(6)	3.4(1)
C(7)	0.4915(4)	0.2261(4)	0.2579(6)	3.3(1)
C(8)	0.5404(5)	0.2130(5)	0.3736(7)	4.9(2)
C(9)	0.6287(6)	0.1800(5)	0.3667(8)	6.9(2)
C(10)	0.6671(5)	0.1593(6)	0.2432(9)	7.8(2)
C(11)	0.6192(5)	0.1717(6)	0.1305(8)	7.0(2)
C(12)	0.5291(5)	0.2058(5)	0.1355(7)	4.9(2)
C(13)	0.0706(4)	0.2709(3)	0.4407(5)	2.8(1)
C(14)	0.0838(4)	0.2566(4)	0.5671(6)	3.6(1)
C(15)	−1.0202(5)	0.7170(4)	0.3397(6)	4.1(1)
C(16)	−0.0562(5)	0.3240(4)	0.6283(7)	4.7(2)
C(17)	−0.0695(5)	0.3384(4)	0.5009(7)	5.0(2)
C(18)	−0.0047(4)	0.3132(4)	0.4071(6)	3.7(1)
C(19)	0.2331(4)	0.0519(3)	0.2724(5)	2.9(1)
C(20)	0.1608(5)	−0.0064(4)	0.3081(6)	4.3(1)
C(21)	0.1779(6)	−0.0906(5)	0.3124(7)	5.8(2)
C(22)	0.2674(6)	−0.1150(4)	0.2813(7)	5.3(2)
C(23)	0.3383(5)	−0.0586(4)	0.2417(7)	5.3(2)
C(24)	0.3221(4)	0.0271(4)	0.2360(6)	4.1(1)
C(25)	0.0131(4)	0.3266(3)	0.0698(5)	2.9(1)
C(26)	−0.0798(4)	0.2841(4)	0.0005(6)	4.1(1)
C(27)	−0.1550(5)	0.3319(5)	−0.0079(7)	5.4(2)
C(28)	−0.1385(5)	0.4229(4)	0.0515(6)	4.8(2)
C(29)	−0.0471(5)	0.4646(4)	0.1207(7)	5.0(2)
C(30)	0.0299(4)	0.4162(4)	0.1297(6)	4.1(1)
C(31)	0.1253(4)	0.0762(3)	−0.1002(5)	2.9(1)
C(32)	0.1191(4)	−0.0057(4)	−0.0722(6)	3.8(1)
C(33)	0.1026(5)	−0.0806(4)	−0.1785(7)	4.6(2)
C(34)	0.0962(4)	−0.0741(4)	−0.3106(7)	4.5(2)
C(35)	0.1032(5)	0.0078(5)	−0.3375(6)	4.8(2)
C(36)	0.1176(5)	0.0845(4)	−0.2306(6)	4.1(1)
C(37)	0.3206(4)	0.4844(3)	0.1532(5)	2.8(1)
C(38)	0.2913(4)	0.5362(4)	0.2664(6)	3.7(1)
C(39)	0.3258(5)	0.6271(4)	0.3027(7)	4.5(2)
C(40)	0.3881(5)	0.6660(4)	0.2248(7)	4.7(2)
C(41)	0.4151(5)	0.6142(4)	0.1108(7)	4.4(2)
C(42)	0.3827(4)	0.5245(4)	0.0753(6)	3.7(1)
C(43)	0.3400(4)	0.2232(4)	−0.1318(5)	2.9(1)
C(44)	0.3605(4)	0.1381(4)	−0.1495(6)	3.8(1)
C(45)	0.3775(5)	0.0907(4)	−0.2773(6)	4.6(2)
C(46)	0.3742(5)	0.1292(5)	−0.3840(6)	5.0(2)
C(47)	0.3531(5)	0.2146(5)	−0.3652(6)	4.9(2)
C(48)	0.3364(4)	0.2624(4)	−0.2379(5)	3.8(1)

Anisotropically refined atoms are given in the form of the equivalent isotropic displacement parameter defined as: $(4/3)[a^2\beta_{11}+b^2\beta_{22}+c^2\beta_{33}+ab(\cos\gamma)\beta_{12}+ac(\cos\beta)\beta_{13}+bc(\cos\alpha)\beta_{23}]$.

TABLE 4. Positional parameters and their e.s.d.s for $[Ru_2[(tol)NNN(tol)]_4 \cdot CH_3CN]BF_4$

Atom	x	y	z	B (Å^2)[a]
Ru(1)	0.250	0.05305(7)	0.250	3.38(3)
Ru(2)	0.250	0.19418(7)	0.250	3.52(4)
N(1)	0.2780(6)	0.0569(5)	0.0980(6)	3.5(2)
N(2)	0.3016(6)	0.1215(6)	0.0501(6)	4.3(2)
N(3)	0.2963(6)	0.1875(5)	0.1022(6)	3.8(2)
N(4)	0.0991(6)	0.0565(5)	0.2214(6)	3.6(2)
N(5)	0.0523(6)	0.1224(6)	0.1966(6)	4.2(2)
N(6)	0.1040(7)	0.1880(5)	0.2038(6)	3.9(2)
N(7)	0.250	0.3209(9)	0.250	5.4(4)
C(1)	0.2876(8)	−0.0126(6)	0.0354(7)	3.8(3)
C(2)	0.235(1)	−0.0793(7)	0.063(1)	5.9(3)
C(3)	0.245(1)	−0.1480(8)	0.009(1)	6.8(4)
C(4)	0.307(1)	−0.1541(7)	−0.0738(9)	5.4(3)
C(5)	0.359(1)	−0.0871(9)	−0.101(1)	7.2(4)
C(6)	0.350(1)	−0.0172(7)	−0.0472(9)	5.9(4)
C(7)	0.318(1)	−0.2312(8)	−0.131(1)	8.4(5)
C(8)	0.3351(8)	0.2532(6)	0.0425(8)	4.2(3)
C(9)	0.4315(9)	0.2491(7)	0.0064(9)	5.0(3)
C(10)	0.471(1)	0.3104(8)	−0.050(1)	6.2(4)
C(11)	0.416(1)	0.3774(9)	−0.0689(9)	6.6(4)
C(12)	0.320(1)	0.3801(9)	−0.033(1)	7.3(4)
C(13)	0.277(1)	0.3186(7)	0.023(1)	5.4(3)
C(14)	0.459(1)	0.4444(9)	−0.131(1)	11.4(6)
C(15)	0.0367(8)	−0.0126(6)	0.2132(8)	3.7(3)
C(16)	0.066(1)	−0.0799(8)	0.263(1)	5.7(4)
C(17)	0.012(1)	−0.1491(7)	0.254(1)	6.0(4)
C(18)	−0.073(1)	−0.1532(7)	0.196(1)	5.1(3)
C(19)	−0.101(1)	−0.087(1)	0.149(1)	6.8(4)
C(20)	−0.048(1)	−0.0157(8)	0.156(1)	5.8(4)
C(21)	−0.128(1)	−0.2310(8)	0.187(1)	8.8(5)
C(22)	0.0431(7)	0.2528(6)	0.1637(9)	3.9(3)
C(23)	0.0070(9)	0.2470(7)	0.0655(9)	5.0(3)
C(24)	−0.048(1)	0.3098(9)	0.026(1)	6.0(4)
C(25)	−0.0679(9)	0.3768(9)	0.082(1)	6.4(4)
C(26)	−0.032(1)	0.3794(9)	0.179(1)	7.3(4)
C(27)	0.025(1)	0.3178(7)	0.2205(9)	5.4(3)
C(28)	−0.129(1)	0.4454(9)	0.039(1)	11.4(6)
C(29)	0.250	0.392(1)	0.250	5.6(5)
C(30)	0.250	0.479(1)	0.250	10.5(9)
B(1)	0.250	0.680(1)	0.250	6.7(8)
F(1)	0.250	0.7610(9)	0.250	13.9(6)
F(2)[b]	0.325(7)	0.651(2)	0.297(6)	13(2)
F(3)[b]	0.269(7)	0.661(2)	0.152(2)	12(1)
F(4)[b]	0.166(5)	0.653(3)	0.27(1)	20(3)
H(1)	0.190(8)	−0.082(6)	0.121(7)	5.1(7)*
H(2)	0.210(8)	−0.192(6)	0.032(7)	5.1(7)*
H(3)	0.402(8)	−0.091(6)	−0.156(8)	5.1(7)*
H(4)	0.379(8)	0.026(6)	−0.063(8)	5.1(7)*
H(5)	0.366(1)	−0.2246(8)	−0.187(1)	11(1)*
H(6)	0.251(1)	−0.2430(8)	−0.158(1)	11(1)*
H(7)	0.340(1)	−0.2752(8)	−0.087(1)	11(1)*
H(8)	0.467(8)	0.201(6)	0.016(7)	5.1(7)*
H(9)	0.522(8)	0.309(6)	−0.062(8)	5.1(7)*
H(10)	0.276(8)	0.414(7)	−0.047(8)	5.1(7)*
H(11)	0.206(8)	0.324(6)	0.046(7)	5.1(7)*
H(12)	0.532(1)	0.4419(9)	−0.118(1)	11(1)*
H(13)	0.432(1)	0.4944(9)	−0.104(1)	11(1)*
H(14)	0.447(1)	0.4420(9)	−0.205(1)	11(1)*
H(15)	0.115(8)	−0.074(6)	0.311(7)	5.1(7)*
H(16)	0.039(9)	−0.184(7)	0.284(8)	5.1(7)*
H(17)	−0.136(8)	−0.082(6)	0.094(7)	5.1(7)*
H(18)	−0.053(8)	0.022(6)	0.104(7)	5.1(7)*
H(19)	−0.191(1)	−0.2238(8)	0.148(1)	11(1)*
H(20)	−0.144(1)	−0.2511(8)	0.255(1)	11(1)*
H(21)	−0.085(1)	−0.2692(8)	0.152(1)	11(1)*
H(22)	0.018(8)	0.206(6)	0.031(8)	5.1(7)*
H(23)	−0.065(8)	0.300(7)	−0.036(8)	5.1(7)*
H(24)	−0.036(8)	0.423(7)	0.209(8)	5.1(7)*
H(25)	0.047(8)	0.324(7)	0.285(8)	5.1(7)*
H(26)	−0.126(1)	0.4322(9)	−0.033(1)	11(1)*
H(27)	−0.096(1)	0.4968(9)	0.051(1)	11(1)*
H(28)	−0.200(1)	0.4483(9)	0.061(1)	11(1)*

[a] Starred atoms were refined isotropically. Anisotropically refined atoms are given in the form of the equivalent isotropic displacement parameter defined as: $(4/3)[a^2\beta_{11}+b^2\beta_{22}+c^2\beta_{33}+ab(\cos\gamma)\beta_{12}+ac(\cos\beta)\beta_{13}+bc(\cos\alpha)\beta_{23}]$. [b] Site modelled as 0.5 F.

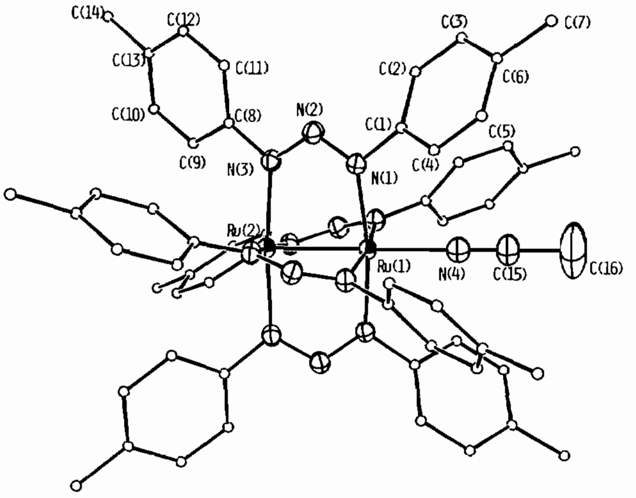

Fig. 1. An ORTEP drawing of $Ru_2(tolNNNtol)_4(CH_3CN)$. For clarity, all of the carbon atoms were given an arbitrary thermal ellipsoid.

The molecular structure of $Ru_2(PhN_3Ph)_4$ (**2**) is shown in Fig. 2, and the principal dimensions are listed in Table 6. The coordination geometry of **2** is exactly the same as that of **4**. The bridging bidentate mode of the PhN_3Ph^- ligand [8] is thus confirmed. The Ru–Ru distance is 2.3994(6) Å, which is a little shorter than that of **4** and 0.014 Å longer than that of $Ru_2(PhN_3Ph)_4POF_4$ [5]. The constancy of the Ru–N interaction is shown by the closeness of the average Ru–N distance (2.032(4) Å) to those of both **1** and **4**. The central portion is also considerably twisted from the eclipsed configuration by the average torsional angle 11.6(2)°, which is related to the dense packing in the crystal (the volume per non-hydrogen atom is 17.4 Å^3 in **2**, and 19.2 Å^3 in **4**).

TABLE 5. Selected bond distances (Å) and angles (°) for $Ru_2[(tol)NNN(tol)]_4 \cdot CH_3CN$

Bond distances					
Ru(1)–Ru(2)	2.407(1)	N(1)–N(2)	1.304(3)	N(4)–C(15)	1.150(9)
Ru(1)–N(1)	2.064(2)	N(1)–C(1)	1.436(4)	C(15)–C(16)	1.481(12)
Ru(1)–N(4)	2.113(6)	N(2)–N(3)	1.314(3)		
Ru(2)–N(3)	2.045(3)	N(3)–C(8)	1.429(4)		
Bond angles					
Ru(2)–Ru(1)–N(1)	85.53(7)	Ru(1)–N(1)–C(1)	125.0(2)	Ru(2)–N(3)–N(2)	122.9(2)
Ru(1)–Ru(2)–N(3)	86.80(6)	N(2)–N(1)–C(1)	110.6(2)	Ru(2)–N(3)–C(8)	125.4(2)
Ru(1)–N(1)–N(2)	123.1(2)	N(1)–N(2)–N(3)	115.7(3)	N(2)–N(3)–C(8)	111.4(3)

Numbers in parentheses are e.s.d.s in the least significant digits.

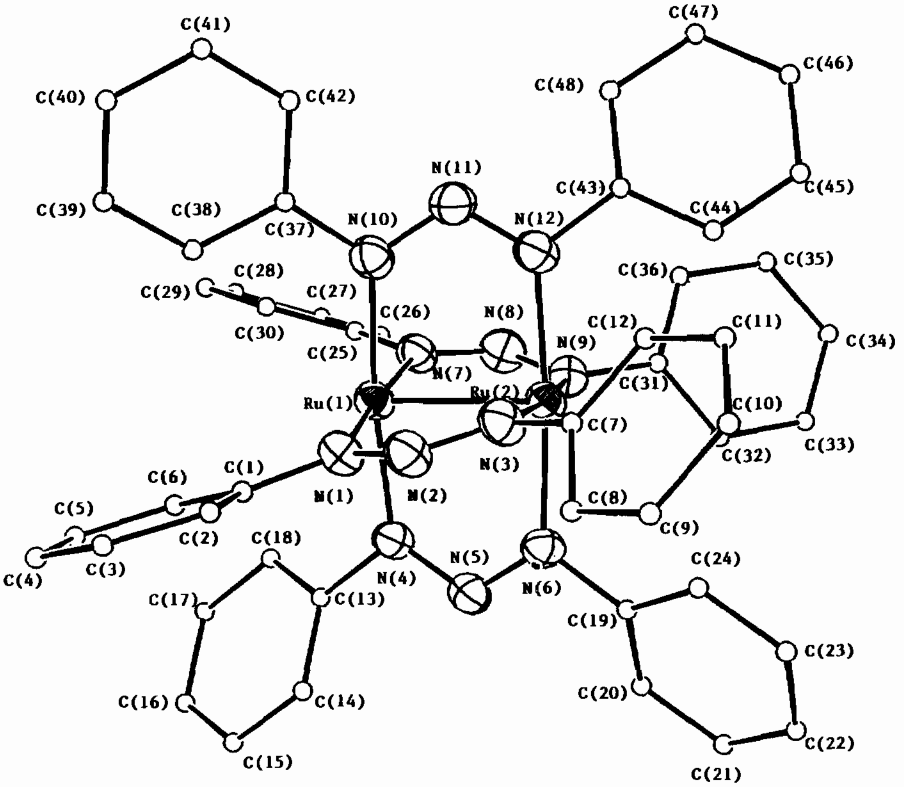

Fig. 2. An ORTEP drawing of $Ru_2(PhNNNPh)_4$. All of the carbon atoms were given an arbitrary thermal ellipsoid.

An ORTEP drawing of the cationic part of **3** is shown in Fig. 3, and the selected bond lengths and angles are deposited in Table 7. In space group *P2/n*, the cation has a rigorous C_2 symmetry with both ruthenium atoms and the three non-hydrogen atoms of axial CH_3CN sitting on the two-fold axis. The average Ru–N distance is again 2.033(8) Å, but the distortion from the ideal eclipsed configuration (the average torsional angle is 6.9(3)°) is less severe than in **2**.

The synthesis and structural characterization of **3** were aimed at determining if the change of Ru–Ru bond length is close to the ideal value corresponding to the removal of an electron from π^{*4}, i.e. 0.07 Å. However, the Ru–Ru distance actually determined is 2.373 Å, which is only 0.045 Å shorter than that of the neutral molecule. The axial ligand CH_3CN is also interacting strongly with the diruthenium core to give a short Ru(2)–N(7) distance (2.131(15) Å). The slight inconsistency between the expectation and the measurement is very unlikely to be caused by the axial ligation, since we have already pointed out in the case of **1** that the axial acetonitrile does not result in the lengthening of the Ru–Ru distance. It is possible that since the previous comparison was made based on the structural data of two diruthenium(II,II) complexes, an additional coulombic repulsion between Ru(III) and Ru(II) would increase the Ru–Ru distance in $[Ru_2(p\text{-}tolN_3p\text{-}tol)_4CH_3CN]^+$ and make the change of the bond length smaller than originally expected.

More direct proof that **3** has a π^{*3} ground state configuration comes from the effective magnetic moment

TABLE 6. Selected bond distances (Å) and angles (°) for $Ru_2(PhN_3Ph)_4$

Bond distances					
Ru(1)–Ru(2)	2.3994(6)	Ru(2)–N(6)	2.018(4)	N(5)–N(6)	1.316(6)
Ru(1)–N(1)	2.028(4)	Ru(2)–N(9)	2.021(4)	N(7)–N(8)	1.308(5)
Ru(1)–N(4)	2.033(4)	Ru(2)–N(12)	2.016(5)	N(8)–N(9)	1.313(7)
Ru(1)–N(7)	2.029(4)	N(1)–N(2)	1.310(6)	N(10)–N(11)	1.310(6)
Ru(1)–N(10)	2.062(4)	N(2)–N(3)	1.313(5)	N(11)–N(12)	1.308(6)
Ru(2)–N(3)	2.045(4)	N(4)–N(5)	1.312(6)		
Bond angles					
Ru(2)–Ru(1)–N(1)	88.1(1)	Ru(1)–Ru(2)–N(12)	87.2(1)	Ru(1)–N(7)–N(8)	124.4(4)
Ru(2)–Ru(1)–N(4)	86.6(1)	Ru(1)–N(1)–N(2)	123.2(3)	N(7)–N(8)–N(9)	115.8(4)
Ru(2)–Ru(1)–N(7)	86.8(1)	N(1)–N(2)–N(3)	115.4(4)	Ru(2)–N(9)–N(8)	123.6(3)
Ru(2)–Ru(1)–N(10)	85.8(1)	Ru(2)–N(3)–N(2)	124.7(3)	Ru(1)–N(10)–N(11)	122.7(3)
Ru(1)–Ru(2)–N(3)	85.6(1)	Ru(1)–N(4)–N(5)	124.6(3)	N(10)–N(11)–N(12)	115.7(4)
Ru(1)–Ru(2)–N(6)	87.7(1)	N(4)–N(5)–N(6)	115.3(4)	Ru(2)–N(12)–N(11)	123.9(3)
Ru(1)–Ru(2)–N(9)	87.5(1)	Ru(2)–N(6)–N(5)	124.2(4)		

Numbers in parentheses are e.s.d.s in the least significant digits.

TABLE 7. Selected bond distances (Å) and angles (°) for $[Ru_2(tolNNNtol)_4(CH_3CN)]BF_4$

Bond distances					
Ru(1)–Ru(2)	2.373(2)	Ru(2)–N(6)	2.032(9)	N(4)–N(5)	1.312(12)
Ru(1)–N(1)	2.027(8)	Ru(2)–N(7)	2.131(15)	N(5)–N(6)	1.303(12)
Ru(1)–N(4)	2.039(8)	N(1)–N(2)	1.295(12)		
Ru(2)–N(3)	2.035(8)	N(2)–N(3)	1.304(12)		
Bond angles					
Ru(2)–Ru(1)–N(1)	88.2(2)	Ru(1)–N(1)–N(2)	123.2(6)	N(4)–N(5)–N(6)	116.7(8)
Ru(2)–Ru(1)–N(4)	88.4(2)	N(1)–N(2)–N(3)	116.5(8)	Ru(2)–N(6)–N(5)	124.5(7)
Ru(1)–Ru(2)–N(3)	86.8(2)	Ru(2)–N(3)–N(2)	124.2(6)		
Ru(1)–Ru(2)–N(6)	87.1(2)	Ru(1)–N(4)–N(5)	122.3(6)		

Numbers in parentheses are e.s.d.s in the least significant digits.

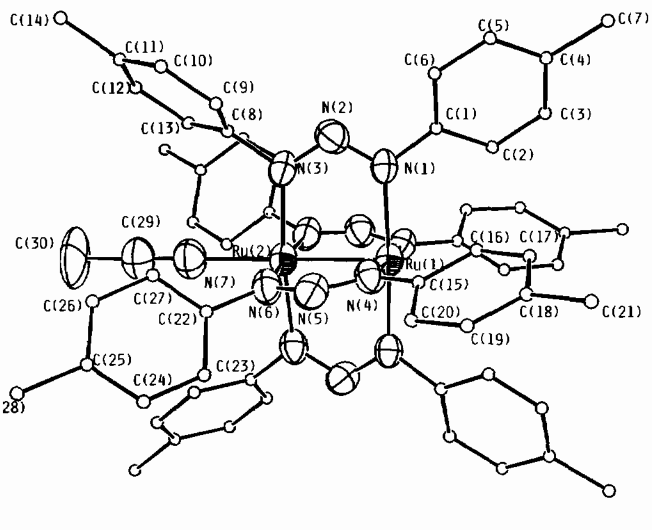

Fig. 3. An ORTEP drawing of $[Ru_2(tolNNNtol)_4(CH_3CN)]^+$.

of 1.88 μ_B which corresponds to the presence of one unpaired electron. Furthermore, even though **3** is a $S=1/2$ system, it is EPR-silent down to 77 K. This behavior can be attributed to the extremely fast relaxation when the unpaired electron is in an orbital-doublet, which means that the ground state is an orbitally degenerate ^2E_g state [17].

The electronic absorption spectrum of **3** also has some interesting features. However, a brief discussion of the spectrum of its parent compound, **4**, is necessary because there are two peaks left unassigned in the original paper. In light of the discussion presented in the work on an analogous compound of **4**, Ru_2(di-*p*-tolylformamidine)$_4$ [6], the intense peak at 327 nm is no doubt the LMCT ($N \rightarrow \delta^*$) band, and the other at 540 nm is by the analogy the metal-localized $\pi^* \rightarrow \delta^*$ transition. The latter is of lower energy than the counterpart in the formamidinato complex, because it has been shown that the δ^*–π^* gap in the diruthenium(II) triazeno complex is about 0.2 eV smaller than that in the diruthenium(II) formamidinato complex [6, 7].

Now for **3** we can assign the transition at 332 nm, without any ambiguity, to the LMCT (lone pair of nitrogen atom to the diruthenium ore) on the basis of the intensity. The transition at 756 nm is tentatively assigned as the $\pi^* \rightarrow \delta^*$ transition. A significant shrinking of the π^*–δ^* gap is suggested by the large red shift (4860 cm^{-1} or 0.60 eV) of this transition from **4** to **3**. Such a shrinking observed in our recent work on the compound $Ru_2(DFM)_4Cl$ is so large that a different ground state configuration $\pi^{*2}\delta^*$ was obtained [18]. The electronic nature of this crossing is still uncertain.

Supplementary material

Complete tables of crystal data, bond distances and angles, anisotropic displacement parameters, observed and calculated structure factors for compounds **1**, **2** and **3** are available from author F.A.C.

Acknowledgements

We thank the National Science Foundation for support. We also acknowledge Dr R. C. Torralba for the assistance in the EPR examination of **3**.

References

1 F. A. Cotton and R. A. Walton, *Multiple Bonds Between Metal Atoms,* Wiley, New York, 1982.

2 F. A. Cotton, V. M. Miskowski and B. Zhong, *J. Am. Chem. Soc., 111* (1989) 6177.

3 (a) F. A. Cotton, T. Ren and J. L. Eglin, *J. Am. Chem. Soc., 110* (1990) 3439; (b) *Inorg. Chem., 30* (1991) 2522.

4 F. A. Cotton and M. Matusz, *J. Am. Chem. Soc., 110* (1988) 5761.

5 F. A. Cotton and M. Matusz, *Chimia, 43* (1989) 167.

6 F. A. Cotton and T. Ren, *Inorg. Chem., 30* (1991) 3675.

7 (a) F. A. Cotton and X. Feng, *Inorg. Chem., 28* (1989) 1180; (b) G. A. Rizzi, M. Casarin, E. Tondello, P. Piraino and G. Granozzi, *Inorg. Chem., 26* (1987) 3406.

8 A. J. Lindsay, G. Wilkinson, M. Motevalli and M. B. Hursthouse, *J. Chem. Soc., Dalton Trans.,* (1987) 2723.

9 A. Bino, F. A. Cotton and P. E. Fanwick, *Inorg. Chem., 18* (1979) 3558.

10 F. A. Cotton, B. A. Frenz, G. Deganello and A. Shaver, *J. Organomet. Chem., 50* (1973) 227.

11 A. C. T. North, D. C. Phillips and F. S. Mathews, *Acta Crystallogr., Sect. A, 24* (1968) 351.

12 (a) G. M. Sheldrick, *SHELXS-86,* Institut für Anorganische Chemie der Universität Göttingen, FRG, 1986; (b) *SHELX-A,* system of computer programs for X-ray structure determination, Cambridge University, Cambridge, UK, 1976.

13 *Enraf-Nonius Structure Determination Package,* Enraf-Nonius Corp., Delft, Netherlands, 1986.

14 K. R. Dunbar, *J. Am. Chem. Soc., 110* (1988) 8247.

15 F. A. Cotton and K. J. Weisinger, *Inorg. Chem., 30* (1991) 871.

16 H. Taube, *Inorg. Chem., 18* (1979) 2216.

17 B. A. Goodman and J. B. Raynor, *Adv. Inorg. Chem. Radiochem., 13* (1970) 135.

18 F. A. Cotton and T. Ren, manuscript in preparation.